# Observation of Ion Tail in ECH/ECCD Plasmas in Helical Devices

Shinji KOBAYASHI, Mitsutaka ISOBE[a], Masaki OSAKABE[a], Hiroyuki MATSUSHITA[a], Masashi KANEKO[a], Tetsuo OZAKI[a], Pavel GONCHAROV[a], Kazunobu NAGASAKI, Yasuo YOSHIMURA[a], Hiroe IGAMI[a], Shin KUBO[a], Takashi SHIMOZUMA[a], Satoshi YAMAMOTO[b], Kazuo TOI[a], Yoshihiko NAGASHIMA[c], Kenji SAITO[a], Hiroshi KASAHARA[a], Katsumi IDA[a], Mikiro YOSHINUMA[a], Sadatsugu MUTO[a], Tohru MIZUUCHI, Hiroyuki OKADA, Katsumi KONDO[d], Kiyoshi HANATANI, Fumimichi SANO and Shoichi OKAMURA[a]

*Institute of Advanced Energy, Kyoto University, Gokasho, Uji, 611-0011, Japan*
*[a]National Institute for Fusion Science, Oroshi-cho, Toki-shi 509-5292, Japan*
*[b]Kyoto University Pioneering Research Unit for Next Generation, Kyoto University, Gokasho Uji 611-0011, Japan*
*[c]RIAM, Kyushu University, Kasuga 816-8580, Japan*
*[d]Graduate School of Energy Science, Kyoto University, Gokasho, Uji, 611-0011, Japan*

The high energy ion tail, having the energy more than five times higher than the bulk temperature, has been observed in the electron cyclotron heating (ECH) and electron cyclotron current drive (ECCD) plasmas of Heliotron J and CHS. The tail temperature of ion increases with decreasing the density and increasing the ECH power. The ion tails appear under the condition of high tail temperature of electrons measured by the soft X-ray charge-coupled-device system. The comparison of the fraction of the ion tail density between CHS and Heliotron J shows that the tail ions are accelerated selectively in the parallel direction to the magnetic field. The high energy electron is a key factor of the formation of the ion tail.

Keywords: Electron cyclotron heating, ion tail, electron tail, anomalous heating, neutral particle analysis

## 1. Introduction

The formation of the ion tail has been observed in the electron heated plasmas, i.e. electron cyclotron heating (ECH) or electron cyclotron current drive (ECCD) plasmas, in several torus devices [1-4]. The rise and decay times of the ion tail have been much shorter than the collisional energy relaxation time between electrons and ions. This phenomenon has been considered to be due to (1) the acceleration by the strong Landau damping of lower-hybrid (LH) waves excited by the parametric three-wave decay process [1] or (2) the anomalous electron-ion coupling because of the slide-away regime of the electron energy distribution [5]. The high energy charge exchange flux was observed experimentally in the X-mode launch from high magnetic field side in the W7-A stellarator [1]. The low-frequency decay wave corresponding to the LH range of frequency was measured with probe, which might be the cause of the ion acceleration. In the TCV tokamak, it was found that the high energy CX flux increased with the current drive efficiency by ECCD [4]. The numerical calculation shows the TCV experiments were in the slide-away regime. An excitation of waves satisfying the dispersion relation of $\boldsymbol{k}\cdot\boldsymbol{v}_i = \omega = k_{\|}v_e$ has been expected due to the slide-away of the electron energy distribution function in Ref. [5].

*author's e-mail:kobayashi@iae.kyoto-u.ac.jp*

In a low magnetic shear helical device, Heliotron J [6], high energy CX flux has been measured in the 70 GHz 2nd harmonic ECH plasmas [7], even the reflection of the launched EC waves has not been controlled. In this paper, we describe the result on the ion tail measurements in the ECH/ECCD plasmas in Heliotron J and Compact Helical System (CHS) [8]. The rise time of the ion tail formation is examined in Heliotron J. The dependence of the tail temperature on the electron density is studied in Heliotron J and CHS. The density of ion tail is investigated from the viewpoint of the normalized ECH power. The mechanism of the formation of the ion tail is discussed by the experimental results obtained in Heliotron J and CHS.

## 2. Experimental results

### 2.1 Heliotron J

The 70 GHz ECH system has been installed in Heliotron J, medium sized ($R_0/a$ = 1.2m/0.17m) helical-axis heliotron device with L/M =1/4 helical coil, where L and M are the pole number of the helical coil and helical pitch respectively [6]. The 2nd harmonic ECH experiments have been carried out using two injection methods; corner section and straight section launch [9]. In the case of the corner section launch, the focused EC

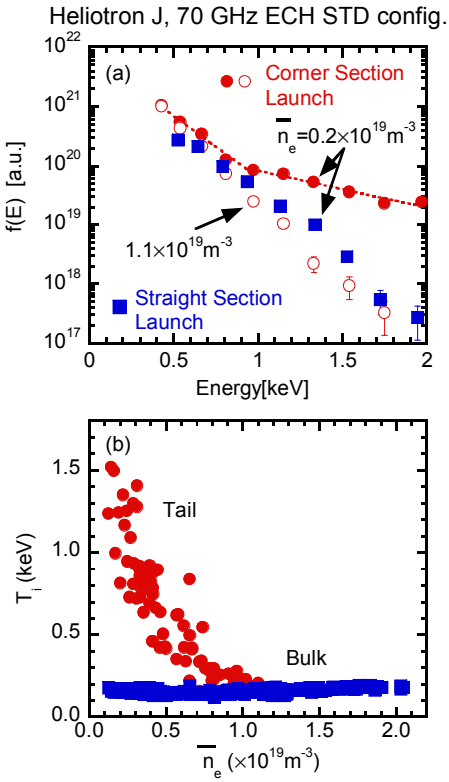


Fig.1 (a) Energy spectra of charge exchange flux obtained in 70 GHz ECH plasmas of Heliotron J and (b) tail and bulk temperature of ion as a function of line-averaged electron density.

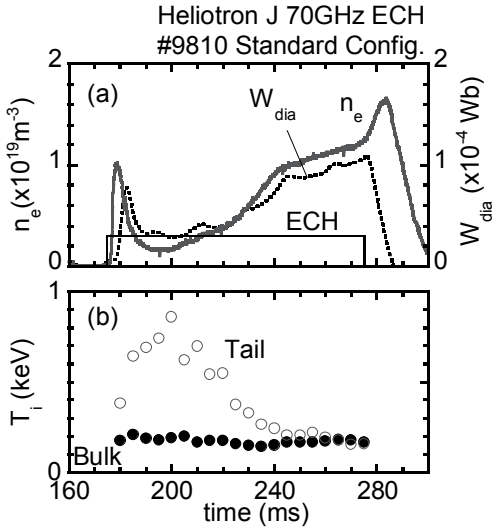


Fig.2 Time evolution of plasma parameters in ECH plasmas of Heliotron J, (a) line-averaged density and stored energy and (b) tail and bulk temperature of ion.

waves using mirror system were launched from the outer torus side of the corner section, where the tokamak-like magnetic field was formed. The non-focused EC waves were launched at the straight section. The gradient of the magnetic field strength at the straight section is small owing to the formation of the quasi-omnigenous magnetic field.

Figure 1(a) shows the CX energy spectrum measured by the CX neutral particle analyzer (CX-NPA) [10] obtained in the standard configuration of Heliotron J. The CX-NPA is E//B type one, whose energy range is from 0.4 to 80 keV for hydrogen and from 0.2 to 40 keV for deuterium, respectively. CX-NPA detected the ions with the pitch angle of 110 degree to the magnetic field in the standard configuration of Heliotron J. In the experiments of the corner section launch under the low density condition at the line-averaged electron density $n_e$ of 0.2 × $10^{19}$ m$^{-3}$, the high energy ion flux was found in the energy range more than five times higher than the bulk ion temperature. The bulk temperature estimated to be 210 eV from the slope of the CX spectrum in the energy range from 0 to 1 keV. A folded spectrum more than 1 keV shows the tail temperature is 710 eV. In the higher density at $n_e$ = 1.1 × $10^{19}$ m$^{-3}$, no clear tail was observed, which shows the tail formation depends on the electron density. The ray tracing calculation of the EC waves shows the absorption profile in the corner section launch is localized at the resonance layer [11]. In the straight section launch, on the contrary, ion tail has not been measured clearly even in the low density condition at $n_e$ = 0.2 × $10^{19}$ m$^{-3}$. A relatively long-path absorption profile was expected by the ray tracing calculation in the straight section launch [9]. It was also found that the tail temperature depended on the injection power of ECH ($P_{ECH}$) in the case of the corner section launch, that is, the tail temperature was 840 eV at the electron density of 0.4 × $10^{19}$ m$^{-3}$ with $P_{ECH}$ of 310 kW, while that at $P_{ECH}$ = 240 kW was 250 eV. These results indicate the focused strong EC waves are favorable to the formation of the ion tail.

Figure 1(b) shows the dependence of the bulk and tail temperatures on the line-averaged electron density. These data were obtained in the ECH injection power of 310 kW in the corner section launch. The tail component was observed in the case that the density was lower than 1.0 × $10^{19}$ m$^{-3}$. The tail temperature increased up to 1.5 keV with decreasing the density. The bulk ion temperature, on the other hand, was not so sensitive to the density in the density range below than 2 × $10^{19}$m$^{-3}$.

Figure 2 (a) and (b) show the time evolution of the line-averaged density, stored energy and tail and bulk ion temperatures measured by the CX-NPA system. The tail temperature increased up to 640 eV by 10 ms at the beginning of the discharge. The decay of the tail temperature was very quick according to the change in the electron density. The electron temperature measured by the SX absorber foil method was about 1 keV. The energy exchange time from electron to ion was about 0.3 sec

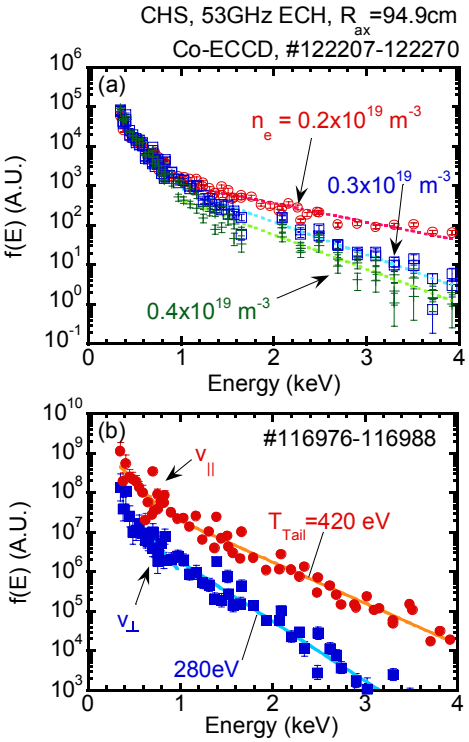


Fig.3 (a) CX energy spectra in 54 GHz ECH plasmas of CHS in $n_e$ = 0.2, 0.3 and 0.4 × $10^{19}$ $m^{-3}$ and (b) comparison of CX energy spectra between parallel and perpendicular velocity .

under the condition, which shows that the formation of ion tail cannot be explained by the classical collision process.

## 2.2. Compact Helical System

CHS is a planner axis helical device ($R_0/a$ = 1.0m/0.2m) with L/N=2/10 helical coil, where N is the toroidal period number [8]. The 53 GHz ECH system in CHS has three steerable mirrors and polarizer to control the injection angle of the EC waves in both toroidal and poloidal directions and the polarity [12]. In CHS, the effect of the X-mode launch from high field side is negligible. The ECCD experiment using the 53 GHz ECH system in CHS is described in Ref. [13].

The CX energy spectrum measured with fast neutral analysis diagnostics (FNA) [14] is shown in Fig. 3 (a) obtained in the ECH plasmas at the line-averaged electron density of 0.2, 0.3 and 0.4 × $10^{19}$ $m^{-3}$, respectively. The ECH injection angle was oblique one and the toroidal current due mainly to ECCD was about 3 kA in the Co-direction under the experimental conditions, which increased the rotational transform. The folded spectra were observed in the energy range more than 0.8 keV. The tail temperature increased with decreasing the density. The density dependence will be discussed later by comparing with the results obtained in Heliotron J.

To examine the velocity distribution of tail ions, the

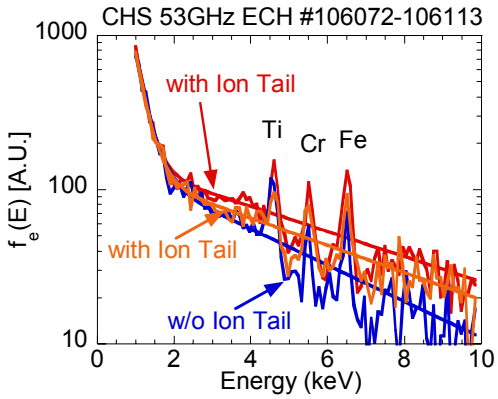


Fig.4 Energy spectrum of electron measured by the SX-CCD system obtained in ECH plasmas of CHS.

parallel and perpendicular velocity components of CX flux to the magnetic field were measured by changing the toroidal angle of FNA. Figure 3 (b) shows the comparison of the CX energy spectra between the parallel and perpendicular directions. These data were obtained in the Co-ECCD plasmas at the electron density of 0.2 × $10^{19}$ $m^{-3}$. The CX flux in the parallel velocity direction was higher than that of the perpendicular one. The bulk and tail temperatures in the parallel direction were 170 and 420 eV, respectively, while those for the perpendicular direction are 160 and 290 eV, respectively. The fraction of ion tail density is defined by the following formula,

$$\int_{Ec}^{5\times Ec} f_{Tail}(E)\,dE \Big/ \left( \int_{0}^{Ec} f_{Bulk}(E)\,dE + \int_{Ec}^{5\times Ec} f_{Tail}(E)\,dE \right) \quad (1)$$

where $f_{Bulk}(E)$, $f_{Tail}(E)$ and $E_c$ are the energy spectra of the bulk and tail ions and the critical tail energy, respectively. When $E_c$ is given by 1 keV, the tail density fraction is 1.3 % for the parallel direction, while that in the perpendicular case is 0.7 %. These results suggest the tail ions are accelerated selectively to the parallel direction. When the injection angle of ECH was varied from Co- to counter direction in CHS, no clear difference was seen in the ion tail flux on the ECH injection angle.

Figure 4 shows the electron energy distribution measured using the pulse height analysis technique with the soft X-ray charge-coupled device (SX-CCD) system in CHS. [15]. An existence of the high energy electron more than 2 keV was confirmed in the low density ECH plasmas. The slope of the electron tail becomes flat when the ion tails are formed, that is, the ion tails appear under the condition that the tail temperature of electron is higher than 4 keV. Thus the high energy electron has a key factor for the formation of the ion tail.

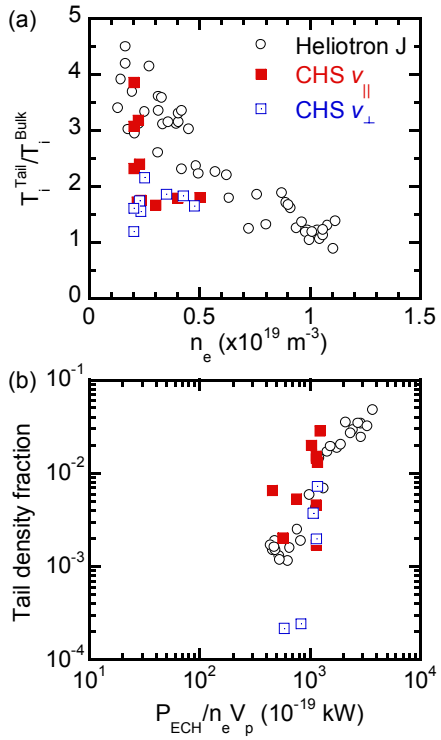


Fig.5 (a) Temperature ratio of tail and bulk ions as a function of electron density and (b) dependence of fraction of ion tail density on the normalized ECH power obtained in Heliotron J and CHS.

## 3. Discussions

In this section, we compare the measurement results of ion tail in Heliotron J and CHS. Figure 5 (a) shows the temperature ratio of tail to bulk ions in Heliotron J and CHS as a function of the electron density. The closed and open squares show the temperature ratios determined by the CX spectra with parallel and perpendicular velocity components in CHS, respectively. In Heliotron J, the CX-NPA has set almost perpendicularly. The temperature ratios in Heliotron J and in the parallel component in CHS increase with decreasing the density. The temperature ratio in the case of the perpendicular component of CHS is lower than the Heliotron J results. This is attributed to the difference in the injection power of ECH between CHS and Heliotron J.

Figure 5 (b) shows the fraction of ion tail density as a function of the ECH injection power normalized by the total electron numbers (electron density times plasma volume $V_p$). The tail density fraction in CHS and Heliotron J increases with the normalized power. A slightly higher fraction of the tail density is obtained at the parallel component in CHS than the others. The perpendicular component in CHS, on the other hand, is in the same order of Heliotron J results.

In order to clarify the effects of the LH-decay wave heating on the ion tail formation, we are planning a X-mode launch from high field side using the ECH system of Large Helical Device [16].

## 4. Summary

We confirmed the formation of the ion tail under the low electron density conditions in ECH plasmas of Heliotron J and CHS. The ion tail formed under the condition that the high energy electron was produced by the focused EC wave. The LH decay wave heating is not considered as the main source of the ion acceleration in Heliotron J and CHS because the effect of the X-mode launch from high field side can be neglected. Although the physical mechanism of the selective acceleration of ions to the parallel direction is still unknown, the high energy electron produced by the focused strong ECH is key factor for the ion tail formation.

## Acknowledgement

One of the authors (S.K.) wishes to thank the experimental members of Heliotron J, CHS and LHD groups. This work is partly supported by the NIFS Collaborative Research Program. (NIFS04KUHL003, NIFS05KUHL007 and NIFS05KLBB003)

## References

[1] V. Erckmann and U. Gasparino, Plasma Phys. Control. Fusion **36**, 1869 (2001).
[2] P. G. Bulyginsky et al, *Control. Fusion Plasma Phys (Proc XI Europ. Conf., Aachen)* **part I** 457, (1983).
[3] Z. A. Pietrzyk et al, Nucl. Fusion **33** 197 (1993)
[4] A.N.Karpushov et al., (*Proc. 30th EPS Conf. Contr. Fusion Plasma.Phys., St. Petersburg 2003*), **27A** p3-123. (2003).
[5] B.Coppi et al., Nucl. Fusion **16** 309 (1976)
[6] F. Sano, et al., Nucl. Fusion **45**, 1557 (2005)
[7] M. Kaneko, et al., *(Proc. 30th EPS Conf Contr. Fusion Plasma Phys., St. Petersburg, 2003)* **27A**, P-3.28 (2003)
[8] S. Okamura et al., Nucl. Fusion **45** 863 (2006)
[9] K. Nagasaki, et al., Nucl. Fusion **45** 13 (2005)
[10] S. Kobayashi et al., (*Proc. 20th IAEA Fusion Energy Conf. Vilamoura, Portugal 2004*) EX/P4-41.
[11] H. Shidara, et al., Fusion Science and Technology, **45** 41 (2004)
[12] Y. Yoshimura et al., Fusion Sci. Tech. **52**, 216 (2007)
[13] K. Nagasaki et al., in this conference
[14] K. Ida, et al., Nucl. Fusion **39** 1649 (1999)
M. Isobe, et al., Nucl. Fusion **41** 1273 (2001)
[15] Y. Liang, et al., Rev. Sci. Instru **71** 3711 (2000)
Y. Liang, et al, Rev. Sci. Instru. **72**, 717 (2001)
[16] Y. Shimozuma et al., Plasma Phys. Control. Fusion **45** 1183 (2003)